Accepted Manuscript

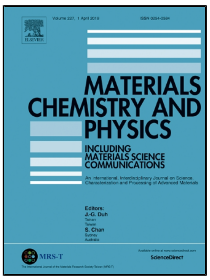

One-Step Production of Pyrene-1-Boronic Acid Functionalized Graphene for Dopamine Detection

Ellie Yi Lih Teo, Gomaa A.M. Ali, H. Algarni, Wilairat Cheewasedtham, Thitima Rujiralai, Kwok Feng Chong

PII:	S0254-0584(19)30325-6
DOI:	10.1016/j.matchemphys.2019.04.029
Reference:	MAC 21549
To appear in:	*Materials Chemistry and Physics*
Received Date:	23 December 2018
Accepted Date:	11 April 2019

Please cite this article as: Ellie Yi Lih Teo, Gomaa A.M. Ali, H. Algarni, Wilairat Cheewasedtham, Thitima Rujiralai, Kwok Feng Chong, One-Step Production of Pyrene-1-Boronic Acid Functionalized Graphene for Dopamine Detection, *Materials Chemistry and Physics* (2019), doi: 10.1016/j.matchemphys.2019.04.029

This is a PDF file of an unedited manuscript that has been accepted for publication. As a service to our customers we are providing this early version of the manuscript. The manuscript will undergo copyediting, typesetting, and review of the resulting proof before it is published in its final form. Please note that during the production process errors may be discovered which could affect the content, and all legal disclaimers that apply to the journal pertain.

ACCEPTED MANUSCRIPT

One-Step Production of Pyrene-1-Boronic Acid Functionalized Graphene for Dopamine Detection

Ellie Yi Lih Teo [a,b,1], Gomaa A.M. Ali [a,c,1], H. Algarni [d,e], Wilairat Cheewasedtham [f], Thitima Rujiralai [f,g], Kwok Feng Chong [a]*

Graphical Abstract:

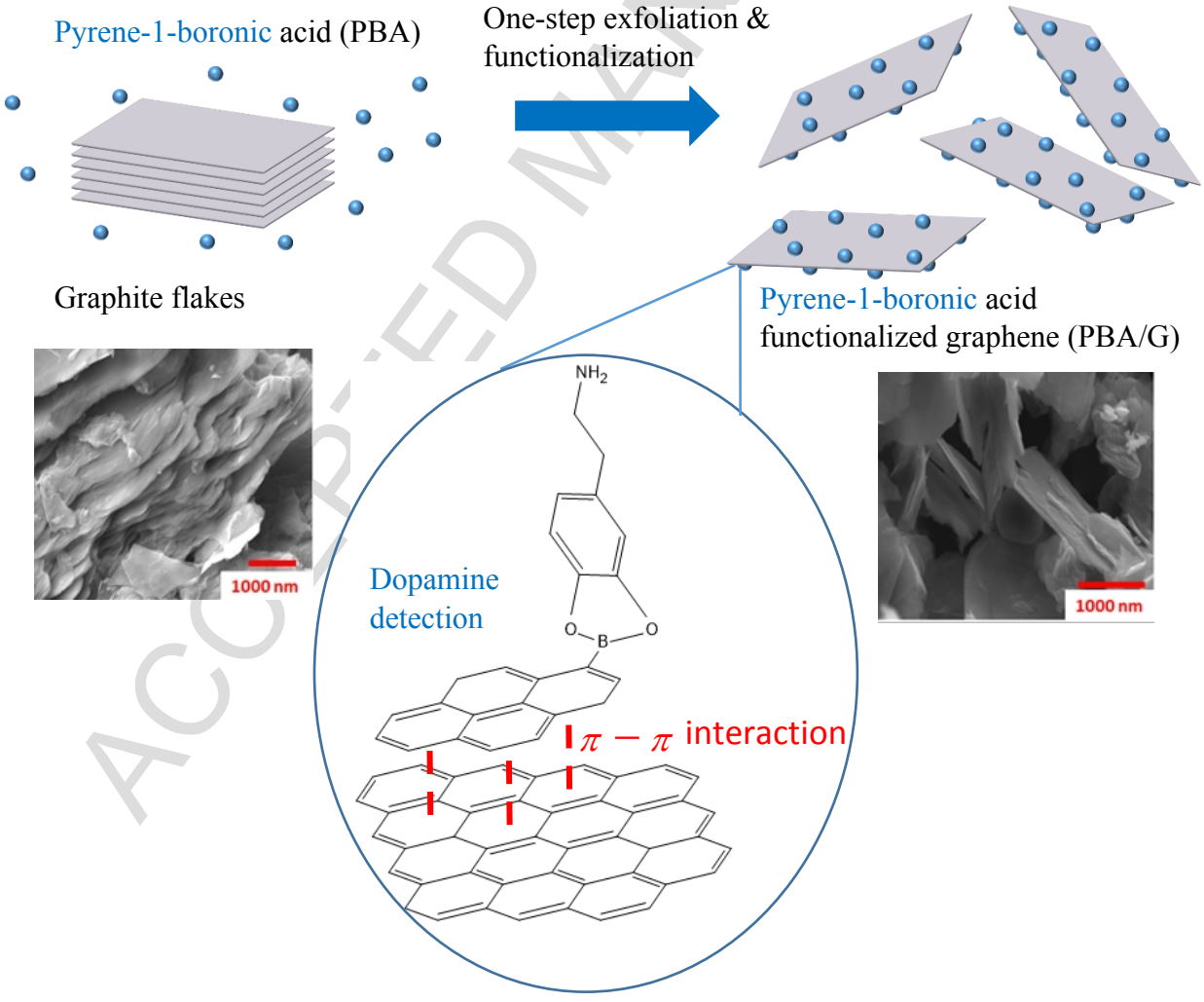

ACCEPTED MANUSCRIPT

One-Step Production of Pyrene-1-Boronic Acid Functionalized Graphene for Dopamine Detection

Ellie Yi Lih Teo [a,b,1], Gomaa A.M. Ali [a,c,1], H. Algarni [d,e], Wilairat Cheewasedtham [f], Thitima Rujiralai [f,g], Kwok Feng Chong [a]*

[a] Faculty of Industrial Sciences & Technology, Universiti Malaysia Pahang, Lebuhraya Tun Razak, 26300 Gambang, Kuantan, Pahang, Malaysia.

[b] R&D Technologies, NGLTech Sdn. Bhd., Suite 8-3, Wisma UOA II, No. 21, Jalan Pinang, 50450 Kuala Lumpur, Malaysia.

[c] Chemistry Department, Faculty of Science, Al-Azhar University, 71524, Assiut, Egypt.

[d] Department of Physics, Faculty of Sciences, King Khalid University, P. O. Box 9004, Abha, Saudi Arabia

[e] Research Center for Advanced Materials Science (RCAMS), King Khalid University, Abha 61413, P. O. Box 9004, Saudi Arabia.

[f] Analytical Chemistry and Environment Research Unit, Division of Chemistry, Department of Science, Faculty of Science and Technology, Prince of Songkla University, Pattani, 94000, Thailand

[g] Department of Chemistry and Center of Excellence for Innovation in Chemistry, Faculty of Science, Prince of Songkla University, Hat Yai, Songkhla, 90112 Thailand

*Corresponding Author: Email: ckfeng@ump.edu.my; Tel: +609-5492403; Fax: +609-5492766

[1] E.Y.L. Teo and G.A.M. Ali are equaly contributed as first author to this work.

ACCEPTED MANUSCRIPT

Abstract

A facile molecular wedging method is used to exfoliate graphite flakes into graphene sheets, with concurrent functionalization to form pyrene-1-boronic acid functionalized graphene (PBA/G). Different techniques are used to characterize the prepared materials such as field emission scanning electron microscope, energy dispersive X-ray analyzer, Raman, Fourier transformed infrared spectroscopy and fluorescence spectroscopy to evaluate their structural and morphological characteristics. The intercalation of PBA into graphite sheets, followed by exfoliation can be observed under electron microscope. Elemental analyses show that the PBA acts more than intercalant, it is functionalized onto the graphene sheets upon exfoliation to form PBA/G. Raman analysis indicates PBA/G has lower number of graphene layers as a results of successful exfoliation by PBA. Electrochemical impedance studies show that the PBA/G possesses high affinity for dopamine through the diol groups interaction, which renders it to have enhanced detection for dopamine.

Keywords: Functionalized graphene, Sensor, Dopamine, Pyrene-1-Boronic acid, Electrochemical impedance.

1. Introduction

Graphene as a two-dimensional material has garnered great research interests due to its outstanding mechanical, optical and physical properties [1-6]. Graphene is an interesting material for sensing applications due its large in-plane conductivity, unique electronic band structure, high specific surface area that can be a platform for molecules interaction [7-10]. The fast

ACCEPTED MANUSCRIPT

heterogeneous electron transfer on graphene surface renders it to be an excellent material for electrochemical applications, therefore it is used widely for the construction of electrochemical sensors [11-14].

Currently, chemical exfoliation [15-17], epitaxial growth on silicon carbide [18], micromechanical cleavage [19] and electrochemical exfoliation [20, 21] are the common approaches to produce graphene sheets. Out of these, chemical exfoliation is deemed as the most effective and economical way to prepare graphene sheets from bulk graphite [20], in which involves the multiple oxidation and reduction process. The major drawback for this approach is the huge consumption of oxidizing agents and acidic solutions, in which poses an environmental issue for its disposal. Furthermore, different applications may require different surface functionalities of graphene sheets and this can only be achieved by additional functionalization steps after the production of graphene. Accordingly, it is of high demand to develop a simple yet efficient method to produce the functionalized graphene sheets.

Dopamine is a catecholamine neurotransmitter in the nervous system, which has a critical role in learning and memory [22-24]. Its low concentration or abnormal metabolisms may lead to some diseases, such as Parkinson disease, epilepsy and senile dementia. Therefore, its monitoring is essential for the correct administration of appropriate drug. Due to its electrochemical active properties, electrochemical detection was proven to be an effective approach for high accuracy and low cost monitoring system for dopamine.

In this work, molecular wedging is used to exfoliate graphite into graphene sheets where pyrene-1-boronic acid (PBA) simultaneously intercalates and functionalizes the graphene sheets (PBA/G). PBA is selected in this work as the pyrene structure resembles graphene basal-plane structure in which interlayer intercalation could be done, in addition to the possible π-π interactions for

ACCEPTED MANUSCRIPT

functionalization [25, 26]. The boronic acid in PBA possesses reversible boronic acid-diol interaction with the forming of boronate ester, which is widely used for the selective binding of saccharides molecules. The prepared materials were characterized using field emission scanning electron microscope (FESEM), energy dispersive X-ray analyzer (EDX), Fourier transformed infrared spectroscopy (FTIR) and fluorescence spectroscopy to evaluate their structural and morphological characteristics. The practicability of PBA/G as biomolecule sensor is tested by the electrochemical impedance spectroscopy (EIS) analysis of dopamine.

2. Experimental

Graphite flakes (100 mg, 99%, Sigma-Aldrich) and different amounts of PBA (16.5, 25, 33 and 50 mg, 95%, Sigma-Aldrich) were first dispersed in 50 mL of ethanol (99.5%, Sigma-Aldrich), followed by sonication for 45 min. Deionized water (200 mL) was later added into the dispersion and it was further sonicated for 4 h. The dispersion was centrifuged, washed, filtered and dried to obtain PBA functionalized graphene (PBA/G). The samples were termed according to their respective PBA:Graphite mass ratio. For example, PBA/G_2 indicates the PBA:Graphite mass ratio of 1:2. Sample surface morphology and elemental composition were studied by a field emission scanning electron microscope (FESEM; JEOL 1525) and energy dispersive X-ray analyzer (EDX), respectively. Raman spectra for the materials under study were obtained using a Raman microscope (Renishaw; inVia) with 2.33 eV (532 nm) laser energy. Fourier transformed infrared spectroscopy (FTIR) was conducted by Perkin Elmer Spectrum 100 spectrometer in the frequency range of 400-4000 cm^{-1} to analyze the functional groups. The fluorescence emission spectra were recorded using fluorescence spectrophotometer (Tecan Infinite 200 Pro).

ACCEPTED MANUSCRIPT

The glassy carbon electrode (GCE) was polished successively with different alumina powders (1.0, 0.3 and 0.05 μm), washed and dried in vacuum. To prepare PBA/G electrode, 10 μL of PBA/G aqueous suspension (1 mg mL^{-1}) was drop casted onto the GCE and then vacuum dried. For dopamine detection, PBA/G electrode was incubated in dopamine solution for 45 min, followed by rinsing with deionized water. The PBA/G electrode was later connected as a working electrode to a frequency response analyzer (AUTOLAB PGSTAT M101), with Pt wire as the counter electrode and Ag/AgCl as the reference electrode. Electrochemical impedance spectroscopy (EIS) was conducted at open circuit potential (OCP) in 0.1 M KCl electrolyte containing 0.5 mM $K_3[Fe(CN)_6/K_4Fe(CN)_6]$ as redox probe. The impedance data was analysed and fitted by equivalent circuit, with the charge transfer resistance values as the response for calibration curve. The process of PBA/G synthesis from graphite and its application as electrode for dopamine detection can be illustrated as Figure 1.

3. Results and discussion

Figure 1 shows the exfoliation begins with the PBA interaction with hydrophobic graphite sheets through its hydrophobic pyrene groups. The sonication process assists the intercalation of PBA at the edges of graphite sheets. Upon addition of water, the solubility of hydrophobic PBA in the solution decreases, forcing the PBA to wedge into the hydrophobic graphite sheets interlayer, under the assistance of sonication. This process continues until the whole graphite sheets interlayer is wedged by PBA molecules and the sheets are separated from each other, forming graphene sheets. Interesting to note that the π-π aromatic interaction between graphene sheets and PBA enables functionalization process occurs simultaneously during the wedging process, thus forming PBA/G. The surface morphology is investigated by FESEM as shown in Figures 2a to 2c. It can

ACCEPTED MANUSCRIPT

be seen that the stacking graphite sheets (Figure 2a) are exfoliated into fewer layers of sheets after the molecular wedging process (Figure 2c). However, control experiment in the absence of PBA (Figure 2b) illustrates the graphite sheets remain stacking. It signifies the role of PBA in the molecular wedging process as the intercalant to exfoliate graphite sheets. The functionalization is confirmed by the elemental analysis (Figure 2d to 2f). Elemental mapping of PBA/G_4 underlines the even distribution of carbon, boron and oxygen atoms, which represents the homogeneous functionalization of PBA onto graphene sheets to form PBA/G.

The carbon-carbon structural information in PBA/G_4 is investigated by Raman spectroscopy, as shown in Figure 3. Raman spectra of graphite and PBA/G_4 exhibit disorder induced (D) band at ca. 1345 cm^{-1} and first–order allowed tangential (G) band at ca. 1571 cm^{-1} due to sp^3 and sp^2 hybridized carbons, respectively [4, 27, 28]. The intensity ratio of D and G bands (I_D/I_G) represents the sp^3/sp^2 carbon ratio and is a measurement of disorder in carbon structure. The I_D/I_G ratios are computed to be 0.11 for PBA/G_4, lower than that for graphite (0.21). It signifies the defect reduction in PBA/G_4 as the PBA could act as a nanographene to repair the defects, which is also in good agreement with other study [29]. The 2D band at ca. 2700 cm^{-1} is due to two-phonon lattice vibration and its shape as well as position are very sensitive to the number of graphene layers. The 2D band for PBA/G_4 (2690 cm^{-1}) is lower than graphite (2703 cm^{-1}), which indicates the lower number of graphene layer as a result of exfoliation during PBA functionalization [29]. In addition, the lower graphene layer in PBA/G_4 is also corroborated by the higher I_{2D}/I_G ratio for PBA/G_4 (0.69), as compared to graphite (0.51).

The successful functionalization is also proven by the FTIR analysis (Figure 4a). Graphite exhibits minor absorption peaks at ca. 3300 and 1650 cm^{-1}, which can be assigned to OH stretching and C=C stretching [30]. The presence of OH could be due to the trace amount of adsorbed water in

ACCEPTED MANUSCRIPT

graphite where C=C is due to the intrinsic chemical bonding in graphite. However, after the molecular wedging process, there is a significant increase in the OH stretching and C=C stretching peaks. This can be associated to the presence of PBA in PBA/G which carries the diol and pyrene groups. Quantitative analysis was performed to study the effect of different PBA concentration in the molecular wedging process. It can be seen from Figure 4a that both the intensities of OH stretching and C=C stretching increase with increasing PBA concentration in the molecular wedging process. The findings can be quantitatively supported by the peak area analysis of both peaks, as shown in Table 1. Higher PBA concentration is accompanied by the higher peak areas for both OH and C=C functional groups, which indicates more PBA is functionalized onto graphene sheets when the concentration of PBA is increased during the molecular wedging process. It also means the amount of functionalized PBA can be easily manipulated. Figure 4b shows the quenching of fluorescence intensity for PBA/G_4. The quenching effect is attributed to the electron transfer between PBA and graphene sheets [29]. Such electron transfer is crucial for electrochemical reaction as the impedance between PBA and graphene sheets is minimized.

Figure 5a shows the Nyquist plots of bare GCE, graphite (after sonication without PBA), and different PBA/G samples in $K_3[Fe(CN)_6/K_4Fe(CN)_6]$ electrolyte, after the electrodes had been exposed to dopamine solution. All the samples manifest simple charge transfer reaction with semicircle at high frequency, followed by straight line at low frequency. This is also parallel to the Bode plot (Figure 5b) to show phase angle increases at lower frequency. The impedance data are fitted to equivalent circuit in Figure 5b inset and charge transfer resistance (R_{ct}) values are used to compare electrode responses. Different samples exhibit different charge transfer behavior which can be observed from their respective R_{ct} values (Figure 5a inset). It is apparent that the R_{ct} values increase dramatically after PBA functionalization onto graphene. This is due to the interaction

ACCEPTED MANUSCRIPT

between dopamine and PBA that imposes higher charge transfer resistance to the electrode. As seen from Figure 1, the interaction between dopamine and PBA can be related to the boronate ester bond forming [31]. It is worth noting that the R_{ct} values increase from PBA/G_2 to PBA/G_4, which is in contrary to the FTIR quantitative analysis to show the higher amount of functionalized PBA from PBA/G_4 to PBA/G_2. Such phenomenon could be associated to the steric effect of higher amount of functionalized PBA [32], which adversely prevents interaction with dopamine. However, the steric effect is insignificant at lower concentration of PBA and the maximum interaction could be observed in PBA/G_4 where highest R_{ct} value is attained. Therefore, subsequent detection of dopamine is conducted on PBA/G_4 electrode. The R_{ct} value is lowest at PBA/G_6 due to the lower amount PBA for the interaction. Different amounts of dopamine are tested on PBA/G_4 electrode (Figure 5c) and the corresponding calibration curve is shown as Figure 5c inset. As expected, higher amount of dopamine leads to higher binding to PBA/G_4 and causes the increase in R_{ct}. A linearity from 7.8 to 125 μM of dopamine detection can be established for PBA/G_4. The Bode plots of PBA/G_4 with different amount of dopamine (Figure 5d) clearly shows that higher amount of dopamine has been interacted to PBA/G_4 where higher phase angle at low frequency is obtained, which can be associated to the capacitance effect of attached dopamine.

The stability and reusability of PBA/G electrode on dopamine sensing were evaluated by removing the attached dopamine after first use by sorbitol and acidic buffer, followed by re-test by dopamine after 30 days (second use). It can be seen from Figure 6 that the R_{ct} values between first and second uses differ by less than 1% which signifies the PBA/G electrode can be reused after removing attached dopamine and stored for 30 days. The interaction between dopamine and PBA was also investigated by running cyclic voltammetry with PBA/G_4 electrode in dopamine solution (Figure 7a). The redox peaks observed can be associated to the dopamine oxidation/reduction, which

ACCEPTED MANUSCRIPT

involves 2-electron process. Figure 7b clearly shows that a linear relationship can be established between redox peaks responses and scan rate, to indicate the surface-controlled redox reaction. Again, this proves the interaction between dopamine and PBA/G, and serves as the basis of developing PBA/G into dopamine sensor.

4. Conclusions

A facile yet efficient approach has been developed to produce pyrene-1-boronic acid (PBA) functionalized graphene from graphite flakes. Molecular wedging method enables the intercalation and exfoliation of graphite sheets and the π-π aromatic interaction allows the functionalization occurs simultaneously. The PBA/G is useful for the electrochemical detection of dopamine where PBA possesses high affinity towards *cis*-diol of dopamine.

Acknowledgments

The authors would like to acknowledge the funding from the Ministry of Education Malaysia in the form of FRGS [RDU170113: FRGS/1/2017/STG07/UMP/01/1], Universiti Malaysia Pahang grant RDU170357 and King Khalid University, the Ministry of Education in Saudi Arabia for supporting this research through grant (RCAMS/KKU/002-18) under research center for advanced material science.

References

[1] F. Bonaccorso, Z. Sun, T. Hasan, A. Ferrari, Graphene photonics and optoelectronics, Nat. Photonics, 4 (2010) 611-622.

ACCEPTED MANUSCRIPT

[2] C. Lee, X. Wei, J.W. Kysar, J. Hone, Measurement of the elastic properties and intrinsic strength of monolayer graphene, Science, 321 (2008) 385-388.

[3] Y. Ito, Y. Tanabe, K. Sugawara, M. Koshino, T. Takahashi, K. Tanigaki, H. Aoki, M. Chen, Three-dimensional porous graphene networks expand graphene-based electronic device applications, Phys. Chem. Chem. Phys., 20 (2018) 6024-6033.

[4] G.A.M. Ali, S.A. Makhlouf, M.M. Yusoff, K.F. Chong, Structural and electrochemical characteristics of graphene nanosheets as supercapacitor electrodes, Rev. Adv. Mater. Sci., 40 (2015) 35-43.

[5] X. Zou, Y. Zhou, Z. Wang, S. Chen, W. Li, B. Xiang, L. Xu, S. Zhu, J. Hou, Free-standing, layered graphene monoliths for long-life supercapacitor, Chem. Eng. J., 350 (2018) 386-394.

[6] A.H. Abdullah, Z. Ismail, A.S. Zainal Abidin, K. Yusoh, Green sonochemical synthesis of few-layer graphene in instant coffee, Mater. Chem. Phys., 222 (2019) 11-19.

[7] P. Suvarnaphaet, S. Pechprasarn, Graphene-Based Materials for Biosensors: A Review, Sensors, 17 (2017) 2161.

[8] A. Ramachandran, S. Panda, S. Karunakaran Yesodha, Physiological level and selective electrochemical sensing of dopamine by a solution processable graphene and its enhanced sensing property in general, Sens. Actuators, B, 256 (2018) 488-497.

[9] M. Hasanzadeh, N. Hashemzadeh, N. Shadjou, J. Eivazi-Ziaei, M. Khoubnasabjafari, A. Jouyban, Sensing of doxorubicin hydrochloride using graphene quantum dot modified glassy carbon electrode, J. Mol. Liq., 221 (2016) 354-357.

[10] K. Chu, F. Wang, X.-l. Zhao, X.-w. Wang, Y. Tian, Electrochemical dopamine sensor based on P-doped graphene: Highly active metal-free catalyst and metal catalyst support, Materials Science and Engineering: C, 81 (2017) 452-458.

ACCEPTED MANUSCRIPT

[11] G. Zhu, P. Gai, L. Wu, J. Zhang, X. Zhang, J. Chen, β-cyclodextrin-platinum nanoparticles/graphene nanohybrids: Enhanced sensitivity for electrochemical detection of naphthol isomers, Chem. Asian J., 7 (2012) 732-737.

[12] K. Wang, Q. Liu, Q.-M. Guan, J. Wu, H.-N. Li, J.-J. Yan, Enhanced direct electrochemistry of glucose oxidase and biosensing for glucose via synergy effect of graphene and CdS nanocrystals, Biosens. Bioelectron., 26 (2011) 2252-2257.

[13] W. Song, D.-W. Li, Y.-T. Li, Y. Li, Y.-T. Long, Disposable biosensor based on graphene oxide conjugated with tyrosinase assembled gold nanoparticles, Biosens. Bioelectron., 26 (2011) 3181-3186.

[14] K. Chu, F. Wang, X.-L. Zhao, X.-P. Wei, X.-W. Wang, Y. Tian, One-step and low-temperature synthesis of iodine-doped graphene and its multifunctional applications for hydrogen evolution reaction and electrochemical sensing, Electrochim. Acta, 246 (2017) 1155-1162.

[15] L. Zhang, J. Liang, Y. Huang, Y. Ma, Y. Wang, Y. Chen, Size-controlled synthesis of graphene oxide sheets on a large scale using chemical exfoliation, Carbon, 47 (2009) 3365-3368.

[16] S. Gu, C.-T. Hsieh, Y.-M. Chiang, D.-Y. Tzou, Y.-F. Chen, Y.A. Gandomi, Optimization of graphene quantum dots by chemical exfoliation from graphite powders and carbon nanotubes, Mater. Chem. Phys., 215 (2018) 104-111.

[17] M. Liu, X. Zhang, W. Wu, T. Liu, Y. Liu, B. Guo, R. Zhang, One-step chemical exfoliation of graphite to 100% few-layer graphene with high quality and large size at ambient temperature, Chem. Eng. J., 355 (2019) 181-185.

ACCEPTED MANUSCRIPT

[18] K.V. Emtsev, A. Bostwick, K. Horn, J. Jobst, G.L. Kellogg, L. Ley, J.L. McChesney, T. Ohta, S.A. Reshanov, J. Röhrl, E. Rotenberg, A.K. Schmid, D. Waldmann, H.B. Weber, T. Seyller, Towards wafer-size graphene layers by atmospheric pressure graphitization of silicon carbide, Nat. Mater., 8 (2009) 203.

[19] F. Bonaccorso, A. Lombardo, T. Hasan, Z. Sun, L. Colombo, A.C. Ferrari, Production and processing of graphene and 2D crystals, Mater. Today, 15 (2012) 564-589.

[20] Y. Hernandez, V. Nicolosi, M. Lotya, F.M. Blighe, Z. Sun, S. De, I.T. McGovern, B. Holland, M. Byrne, Y.K. Gun'Ko, J.J. Boland, P. Niraj, G. Duesberg, S. Krishnamurthy, R. Goodhue, J. Hutchison, V. Scardaci, A.C. Ferrari, J.N. Coleman, High-yield production of graphene by liquid-phase exfoliation of graphite, Nat. Nanotechnol., 3 (2008) 563.

[21] M. Mooste, E. Kibena-Põldsepp, B.D. Ossonon, D. Bélanger, K. Tammeveski, Oxygen reduction on graphene sheets functionalised by anthraquinone diazonium compound during electrochemical exfoliation of graphite, Electrochim. Acta, 267 (2018) 246-254.

[22] H.-B. Wang, Y. Li, G.-L. Dong, T. Gan, Y.-M. Liu, A convenient and label-free colorimetric assay for dopamine detection based on the inhibition of the Cu(ii)-catalyzed oxidation of a 3,3′,5,5′-tetramethylbenzidine–H_2O_2 system, New J. Chem., 41 (2017) 14364-14369.

[23] H.-B. Wang, H.-D. Zhang, Y. Chen, K.-J. Huang, Y.-M. Liu, A label-free and ultrasensitive fluorescent sensor for dopamine detection based on double-stranded DNA templated copper nanoparticles, Sens. Actuators, B, 220 (2015) 146-153.

[24] Y. Li, H.-Y. Bai, Y.-M. Liu, Fluorescent determination of dopamine using polythymine-templated copper nanoclusters, Anal. Lett., 51 (2018) 2868-2877.

ACCEPTED MANUSCRIPT

[25] Y. Zhang, R. Ma, X.V. Zhen, Y.C. Kudva, P. Bühlmann, S.J. Koester, Capacitive sensing of glucose in electrolytes using graphene quantum capacitance varactors, ACS Appl. Mater. Interfaces, 9 (2017) 38863-38869.

[26] M.M. Sari, Fluorescein isothiocyanate conjugated graphene oxide for detection of dopamine, Mater. Chem. Phys., 138 (2013) 843-849.

[27] Y. Yao, J. Gao, F. Bao, S. Jiang, X. Zhang, R. Ma, Covalent functionalization of graphene with polythiophene through a Suzuki coupling reaction, RSC Adv., 5 (2015) 42754-42761.

[28] G.A.M. Ali, M.M. Yusoff, H. Algarni, K.F. Chong, One-step electrosynthesis of MnO_2/rGO nanocomposite and its enhanced electrochemical performance, Ceram. Int., 44 (2018) 7799-7807.

[29] L. Li, X. Zheng, J. Wang, Q. Sun, Q. Xu, Solvent-exfoliated and functionalized graphene with assistance of supercritical carbon dioxide, ACS Sustainable Chem. Eng., 1 (2013) 144-151.

[30] P.E. Marina, G.A.M. Ali, L.M. See, E.Y.L. Teo, E.-P. Ng, K.F. Chong, In situ growth of redox-active iron-centered nanoparticles on graphene sheets for specific capacitance enhancement, Arabian J. Chem., (2016) http://dx.doi.org/10.1016/j.arabjc.2016.1002.1006.

[31] W. Wu, H. Zhu, L. Fan, D. Liu, R. Renneberg, S. Yang, Sensitive dopamine recognition by boronic acid functionalized multi-walled carbon nanotubes, Chem. Commun., 23 (2007) 2345-2347.

[32] A.T. Haedler, H. Misslitz, C. Buehlmeyer, R.Q. Albuquerque, A. Köhler, H.-W. Schmidt, Controlling the π-stacking behavior of pyrene derivatives: influence of H-bonding and steric effects in different states of aggregation, ChemPhysChem, 14 (2013) 1818-1829.

ACCEPTED MANUSCRIPT

One-Step Production of Pyrene-1-Boronic Acid Functionalized Graphene for Dopamine Detection

Ellie Yi Lih Teo [a,b,1], Gomaa A.M. Ali [a,c,1], H. Algarni [d,e], Wilairat Cheewasedtham [f], Thitima Rujiralai [f,g], Kwok Feng Chong [a]*

Highlights:

- Pyrene-1-boronic acid functionalized graphene is prepared using facile molecular wedging method
- Pyrene-1-boronic acid intercalates and functionalizes onto graphene (PBA/G)
- PBA/G possesses high affinity for dopamine
- Electrochemical impedance analyses show enhanced dopamine detection for PBA/G electrode

ACCEPTED MANUSCRIPT

ACCEPTED MANUSCRIPT

One-Step Production of Pyrene-1-boronic Acid Functionalized Graphene for Dopamine Detection

Ellie Yi Lih Teo [a,b,1], Gomaa A.M. Ali [a,c,1], H. Algarni [d,e], Wilairat Cheewasedtham [f], Thitima Rujiralai [f,g], Kwok Feng Chong [a]*

Table 1: FTIR peak areas for graphite and PBA/G with different amounts of PBA.

Figure 1: Schematic presentation molecular wedging process to form PBA/G and its application as electrode for dopamine sensing.

Figure 2: FESEM images of (a) graphite, (b) sonicated graphite without PBA and (c) PBA/G_4; EDX mapping (d-f) for PBA/G_4.

Figure 3: Raman spectra for graphite and PBA/G_4: The inset shows zoomed view of 2D band.

Figure 4: (a) FTIR spectra for graphite and PBA/G with different amounts of PBA; (b) Fluorescence spectra of PBA and PBA/G_4.

Figure 5: (a) Nyquist and (b) Bode plots of PBA/G samples in 125 µM dopamine, insets show the charge transfer resisctance as a function of PBA content and the equivelnt circiut used for data fitting, (c) Nyquist and (d) Bode plots of PBA/G_4 at different concentrations of dopamine, inset shows the calibration curve of PBA/G_4 towards dopamine. Solid lines are the fitting results.

Figure 6: Nyquist plots of PBA/G_4 in 125 µM dopamine after remove PBA and second time use showing stability and reusability.

Figure 7: (a) Cyclic voltamograms of PBA/G_4 at different scan rates in 125 µM dopamine solution; (b) peaks current vs. scan rates.

ACCEPTED MANUSCRIPT

Table 1: FTIR peak areas for graphite and PBA/G with different amounts of PBA.

	Peak area (cm^{-1})	
Samples	-OH stretching	-C=C stretching
Graphite	1569.0	141.0
PBA/G_6	3268.7	1246.7
PBA/G_4	5761.8	1635.5
PBA/G_3	8089.9	2474.9
PBA/G_2	11928.0	3442.5

ACCEPTED MANUSCRIPT

Figure 1

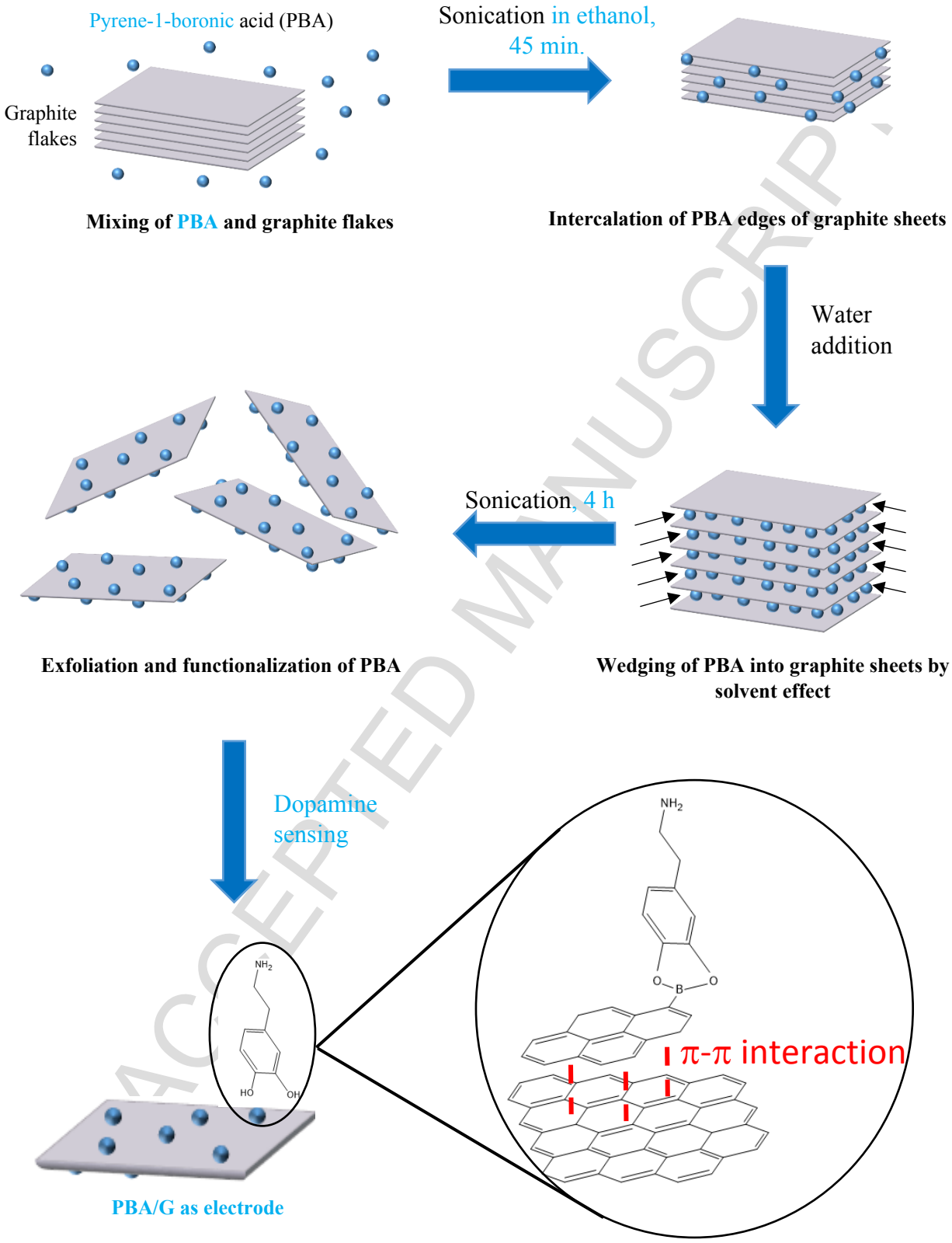

ACCEPTED MANUSCRIPT

Figure 2

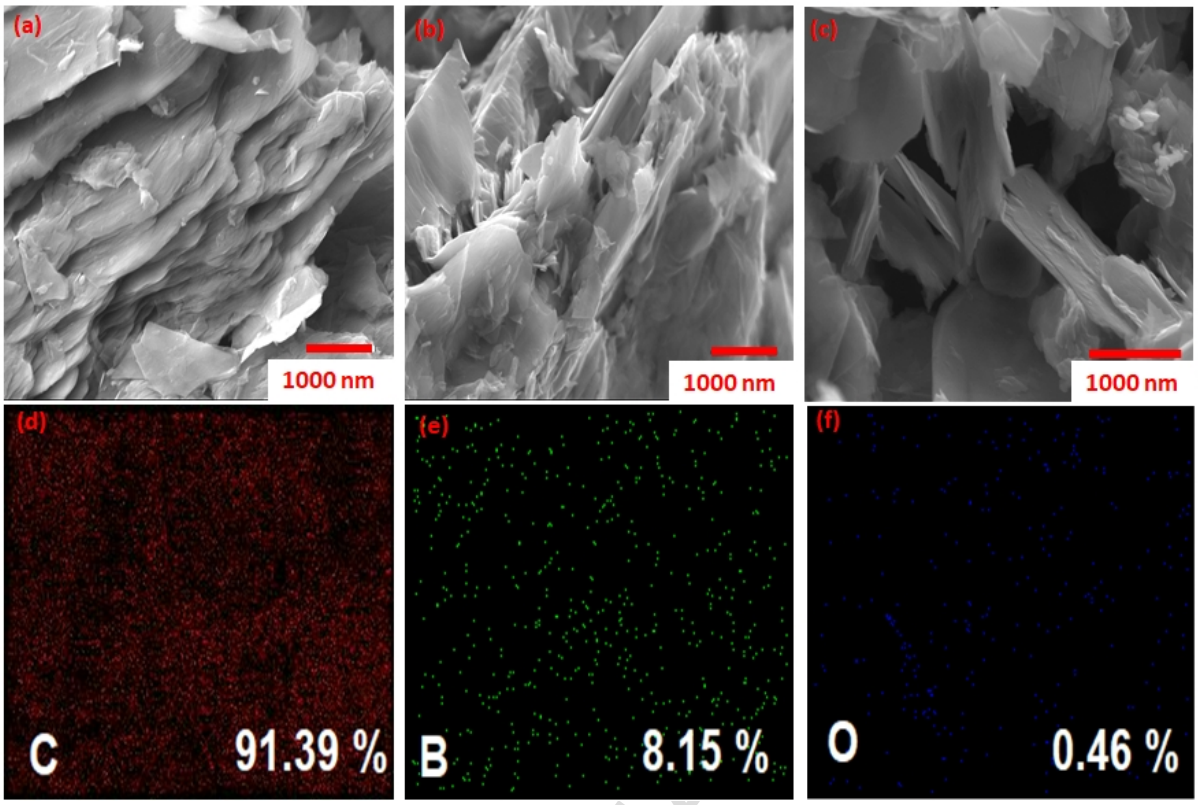

ACCEPTED MANUSCRIPT

Figure 3

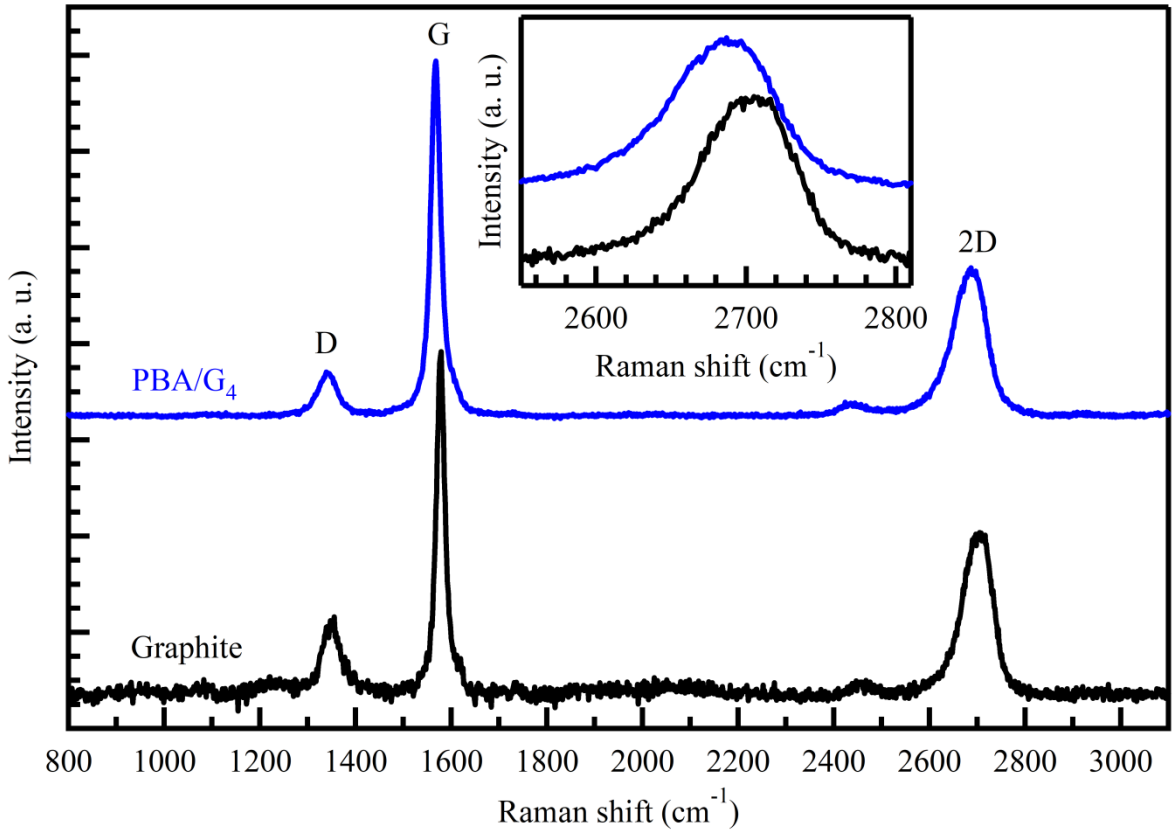

ACCEPTED MANUSCRIPT

Figure 4

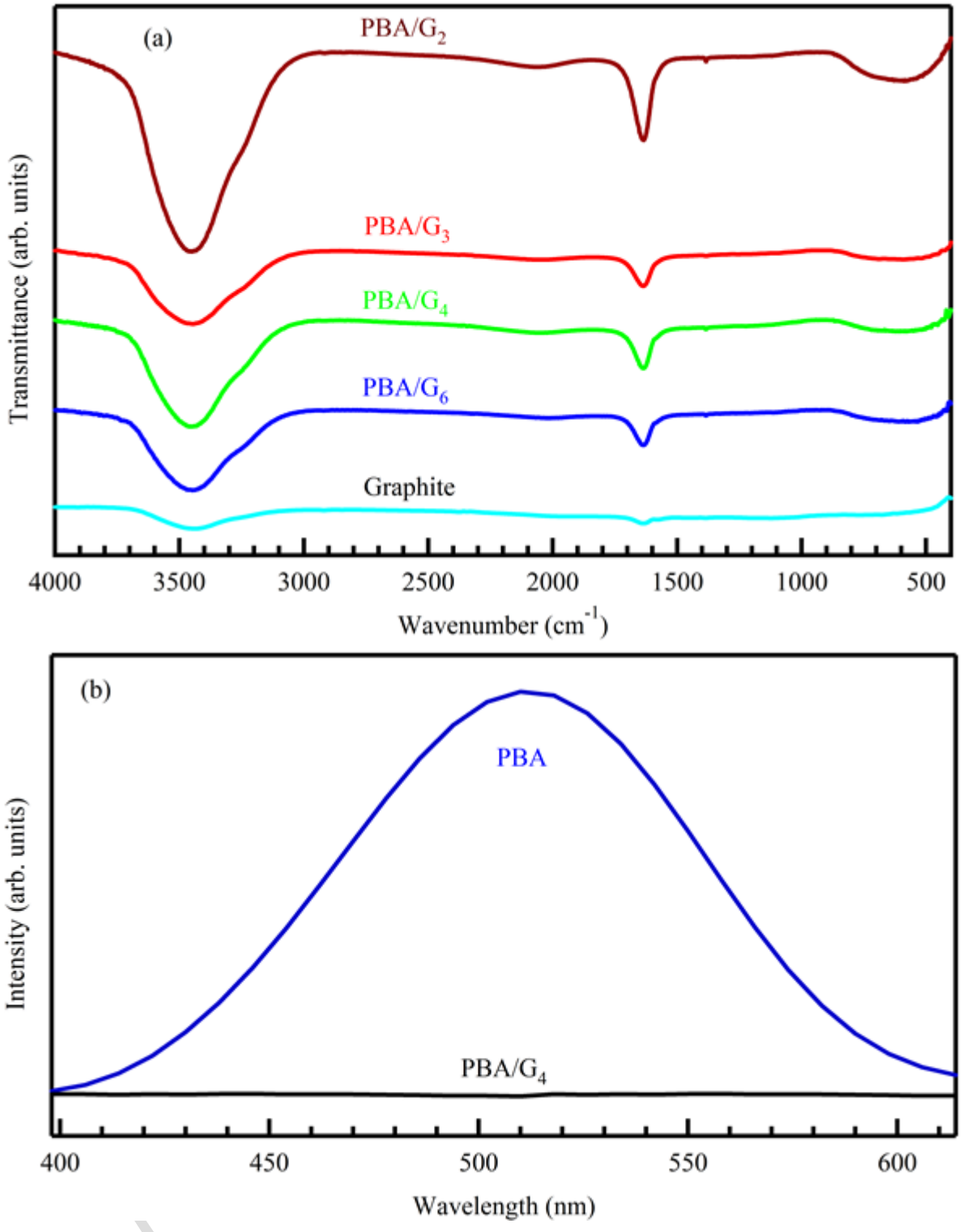
(a)
PBA/G2
PBA/G3
PBA/G4
PBA/G6
Graphite
Transmittance (arb. units)
4000
3500
3000
2500
2000
1500
1000
500
Wavenumber (cm-1)
(b)
PBA
PBA/G4
Intensity (arb. units)
400
450
500
550
600
Wavelength (nm)

Figure 5

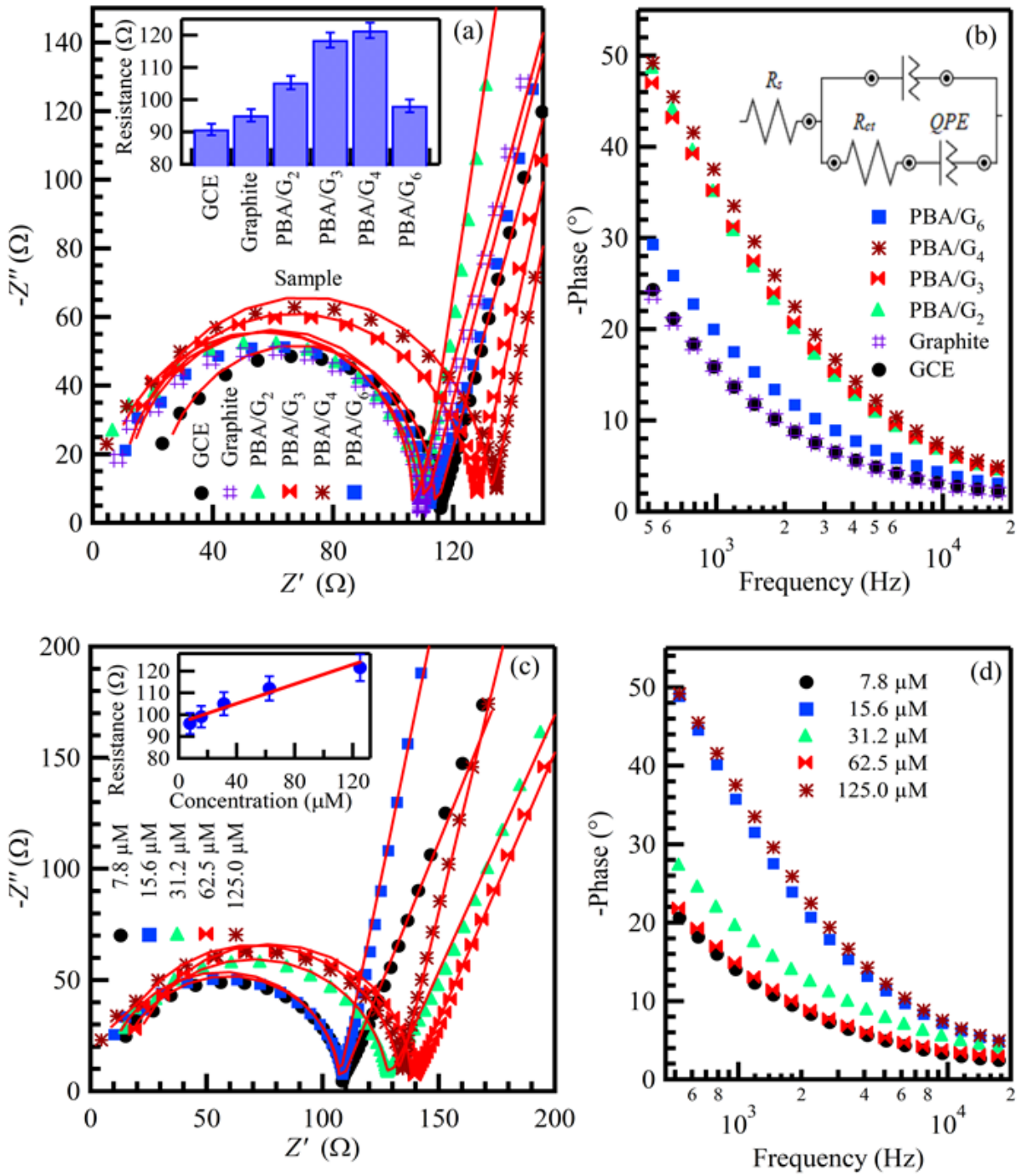
(a)
-Z'' (Ω)
Z' (Ω)
Resistance (Ω)
GCE
Graphite
PBA/G2
PBA/G3
PBA/G4
PBA/G6
Sample
(b)
-Phase (°)
Frequency (Hz)
Rs
Rct
QPE
PBA/G6
PBA/G4
PBA/G3
PBA/G2
Graphite
GCE
(c)
-Z'' (Ω)
Z' (Ω)
Resistance (Ω)
Concentration (μM)
7.8 μM
15.6 μM
31.2 μM
62.5 μM
125.0 μM
(d)
-Phase (°)
Frequency (Hz)
7.8 μM
15.6 μM
31.2 μM
62.5 μM
125.0 μM

Figure 6

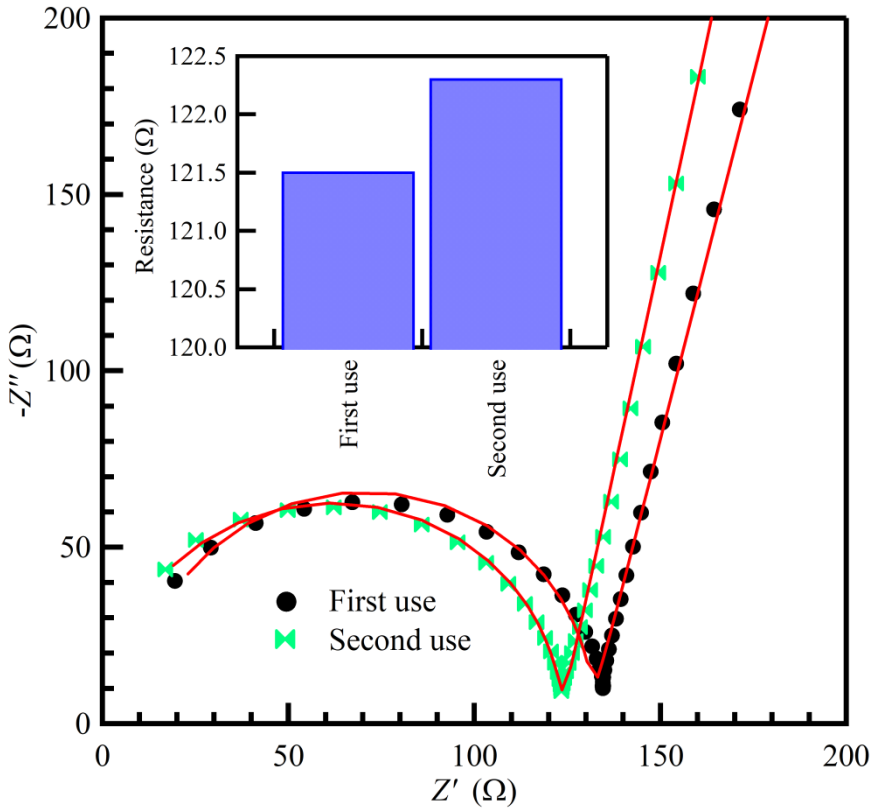

ACCEPTED MANUSCRIPT

Figure 7

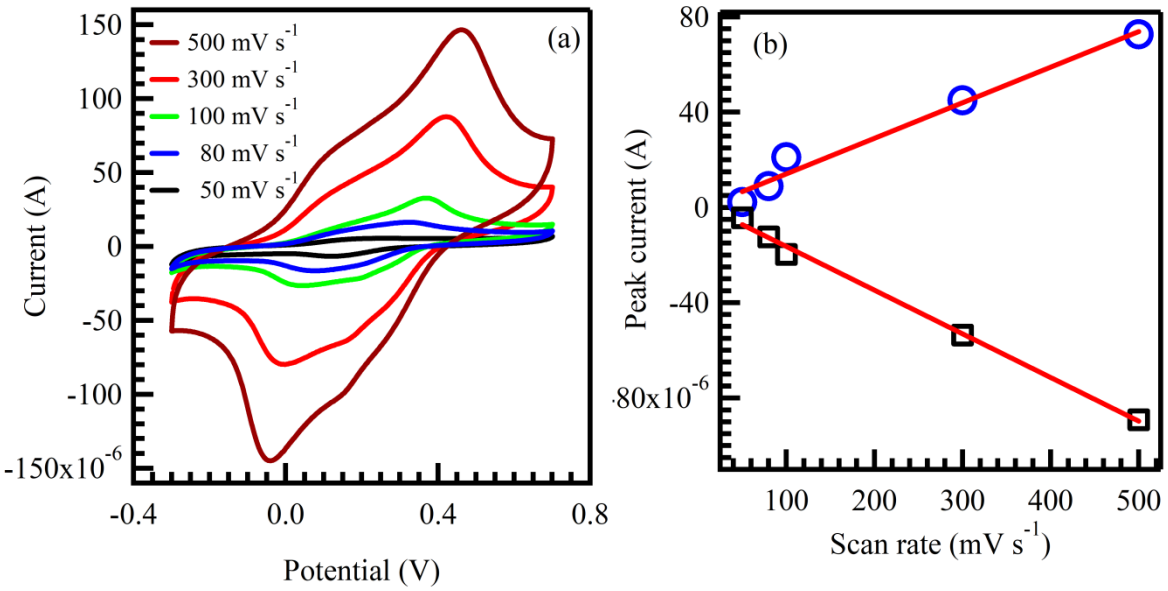

ACCEPTED MANUSCRIPT